

Electronic Supplementary Information

Mesoporous carbon-coated LiFePO₄ nanocrystals co-modified by graphene and Mg²⁺ doping as superior cathode material for high-rate lithium ion batteries

Bo Wang,^{a,b} Binghui Xu,^b Tiefeng Liu,^a Peng Liu,^b Chenfeng Guo,^b Shuo Wang,^c Qiuming Wang,^a Zhigang Xiong,^b Dianlong Wang^{*a} and X. S. Zhao^{*b}

^a Harbin Institute of Technology, School of Chemical Engineering and Technology, Xidazhi Street, 150001 Harbin, China. Fax: 86 45186413721; Tel: 86 451 86413751; E-mail: wangdianlongwbhit@163.com

^b The University of Queensland, Faculty of Engineering, Architecture and Information Technology, School of Chemical Engineering, St Lucia, Brisbane, QLD 4072, Australia. Fax: 61 7 33654199; Tex: 61 7 33469997; E-mail: george.zhao@uq.edu.au

^c Harbin Normal University, College of Chemistry and Chemical Engineering, 150025 Harbin, China. Tel: 86 18345378201; E-mail: wangshuo19900114@163.com

Table of Contents

1. **Fig. S1†** The comparison of the stabilities of ▲ the sucrose/salts solution, ● the GO/sucrose/salts suspension and ■ the GO/sucrose/salts rheological body.
2. **Fig. S2†** TG/DSC curves of LFP precursor after bead milling.
3. **Fig. S3†** Raman spectra of LFP, LFMP, G/LFP and G/LFMP.
4. **Fig. S4†** (a) Nitrogen adsorption/desorption isotherms and pore-size distribution curves of LFP, LFMP, G/LFP and G/LFMP, (b) Nitrogen adsorption/desorption isotherms of thermal reduced graphene.
5. **Fig. S5†** SEM (a) and TEM (c) images of LFP product without bead milling procedure; SEM (b) and TEM (d) images of LFP product experienced bead milling procedure.
6. **Fig. S6†** The TEM images of (a) G/LFP and (b) G/LFMP.
7. **Fig. S7†** Charge/discharge profiles of graphene electrode at 0.2C-0.2D.
8. **Fig. S8†** The charge/discharge profiles of LFP, HLFP and G/LFP at current rates of 0.2C-0.2D.
9. **Fig. S9†** The rate performance of LFP, HLFP and G/LFP from 0.2C-0.2D to 20C-20D.
10. **Fig. S10†** The EIS plots and equivalent circuit of LFP, HLFP and G/LFP.
11. **Fig. S11†** The fitting curves of $-Z''$ and reciprocal square root of the angular frequency at low frequency region of LFP, HLFP, LFMP, G/LFP and G/LFMP.
12. **Fig. S12†** Potential as a function of time of graphene electrode and LFMP electrode at 0.2C-0.2D for both charge (a) and discharge (b) processes.
13. **Table S1†** Results of structural analysis obtained from XRD Rietveld refinement of samples LFP, LFMP, G/LFP and G/LFMP.
14. **Table S2†** The contents of LF(M)P, total carbon including sucrose-pyrolytic carbon and graphene, as well as electronic conductivities of the samples.
15. **Table S3†** Elemental composition of the Mg²⁺ doping samples determined using ICP.
16. **Table S4†** The circuit parameters, D_{Li} , and σ of the samples.

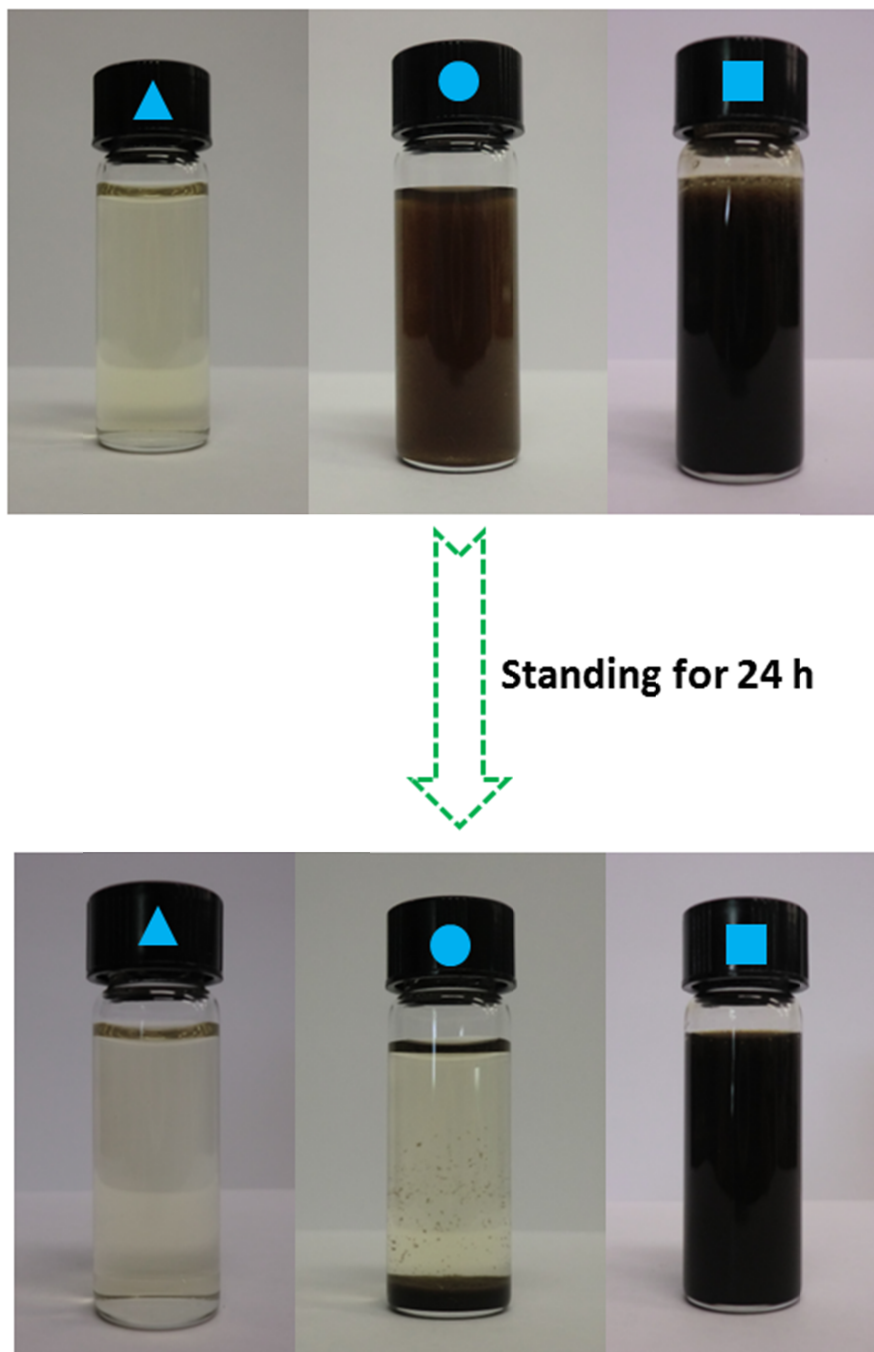


Fig. S1† The comparison of the stabilities of ▲ the sucrose/salts solution, ● the GO/sucrose/salts suspension and ■ the GO/sucrose/salts rheological body. Compared with the GO/sucrose/salts suspension, the GO/sucrose/salts rheological body was more superior for the dispersion of GO due to its much higher viscosity, which could keep stable for at least 24 h that was long enough for evaporating the residual water to get a uniform dry mixture.

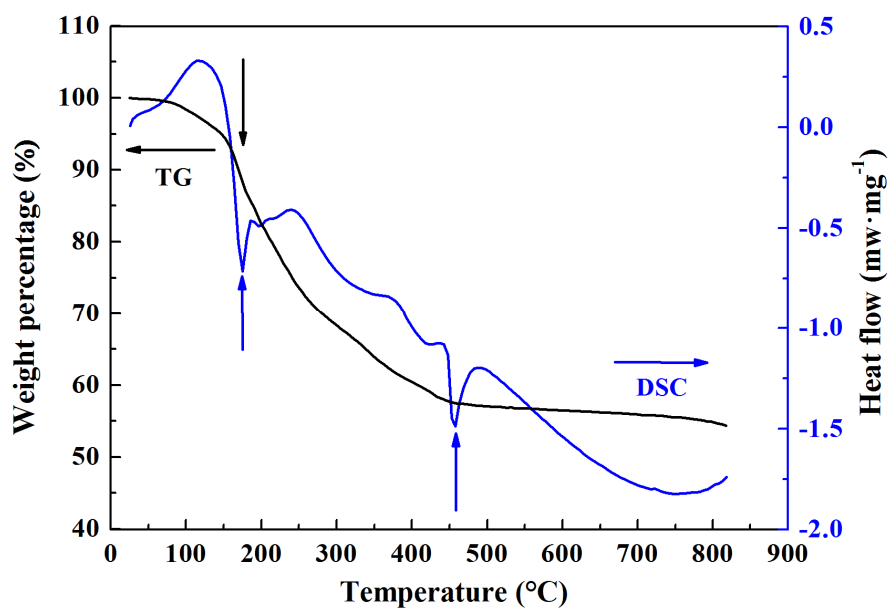


Fig. S2† TG/DSC curves of LFP precursor after bead milling.

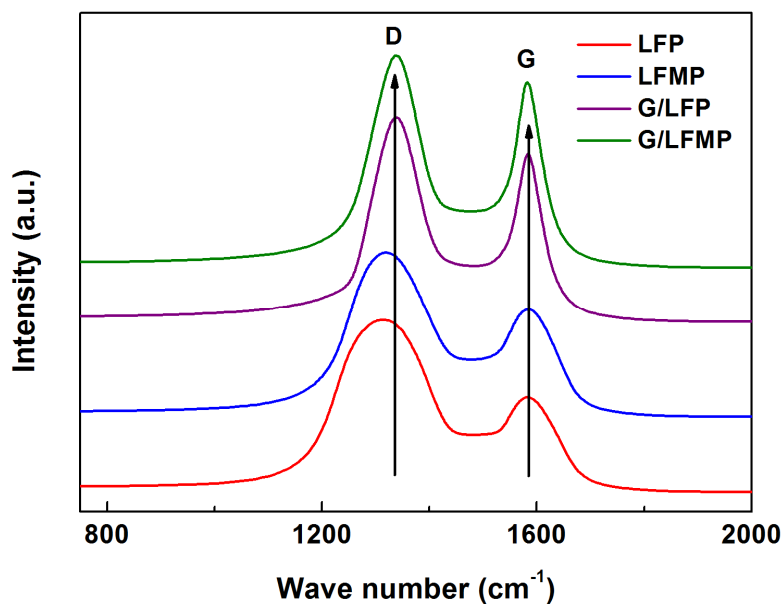


Fig. S3† Raman spectra of LFP, LFMP, G/LFP and G/LFMP.

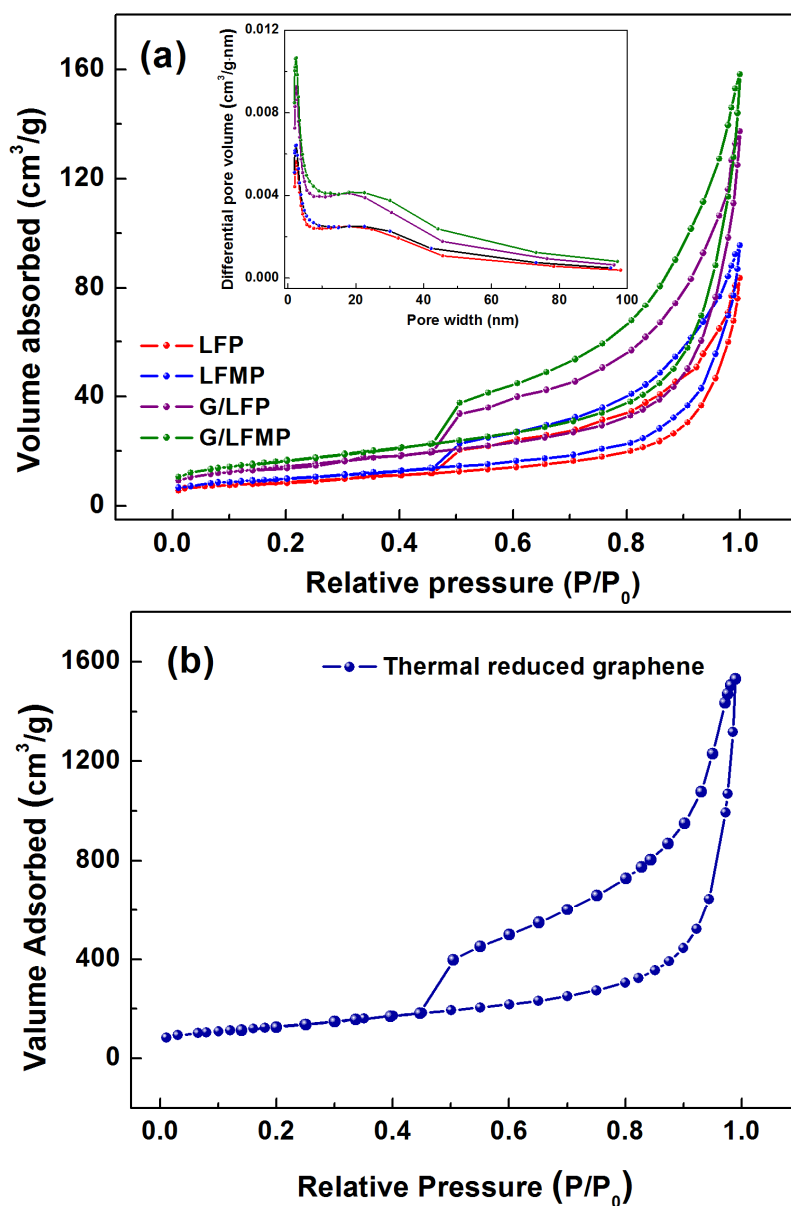


Fig. S4† (a) Nitrogen adsorption/desorption isotherms and pore-size distribution curves of LFP, LFMP, G/LFP and G/LFMP, (b) Nitrogen adsorption/desorption isotherms of thermal reduced graphene.

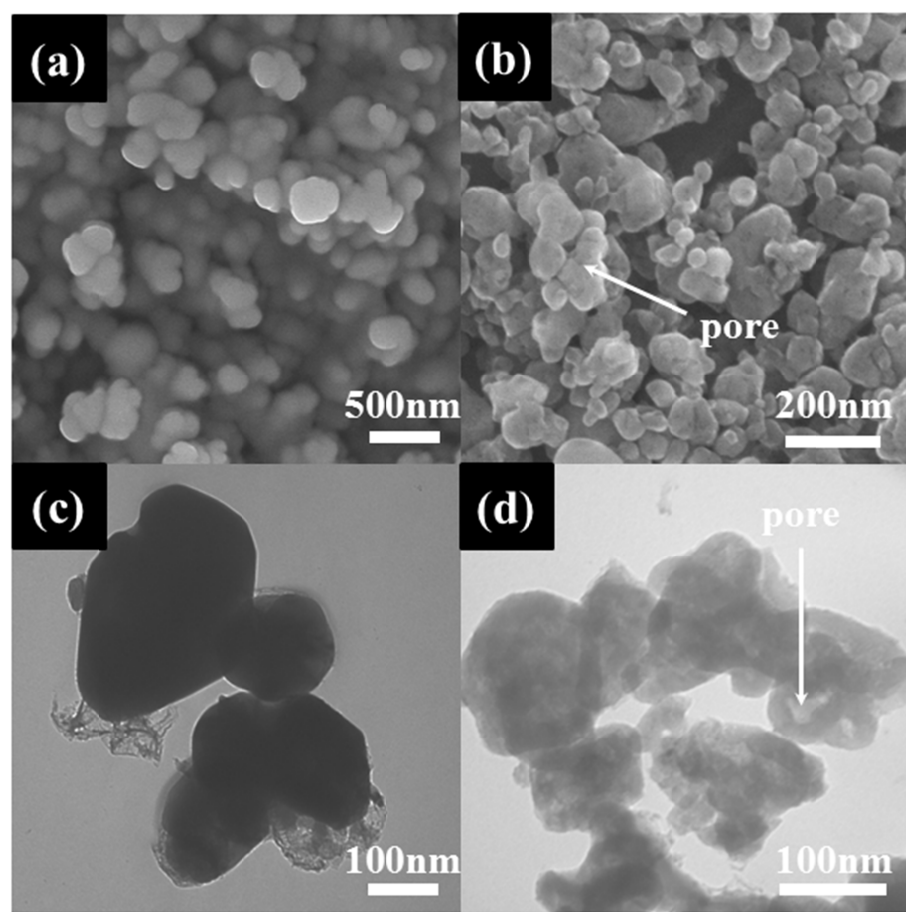


Fig. S5† SEM (a) and TEM (c) images of LFP product without bead milling procedure; SEM (b) and TEM (d) images of LFP product experienced bead milling procedure.

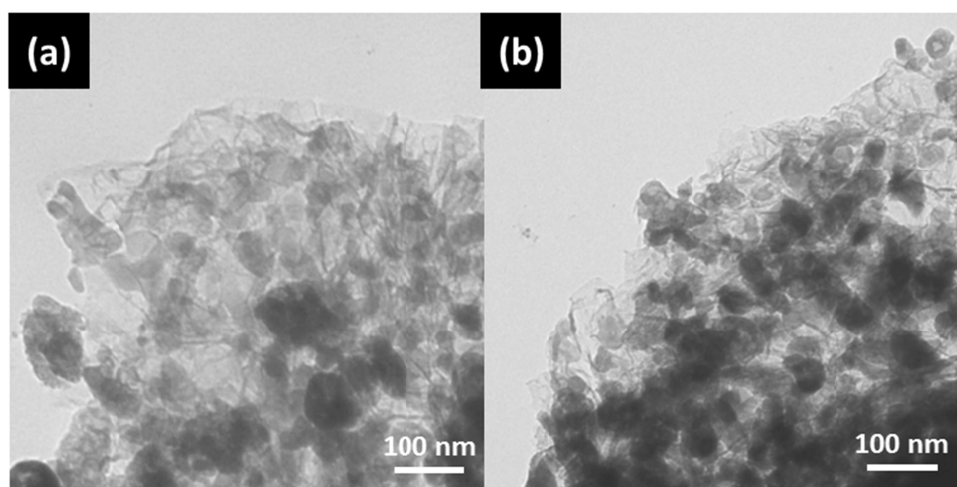


Fig. S6† The TEM images of (a) G/LFP and (b) G/LFMP.

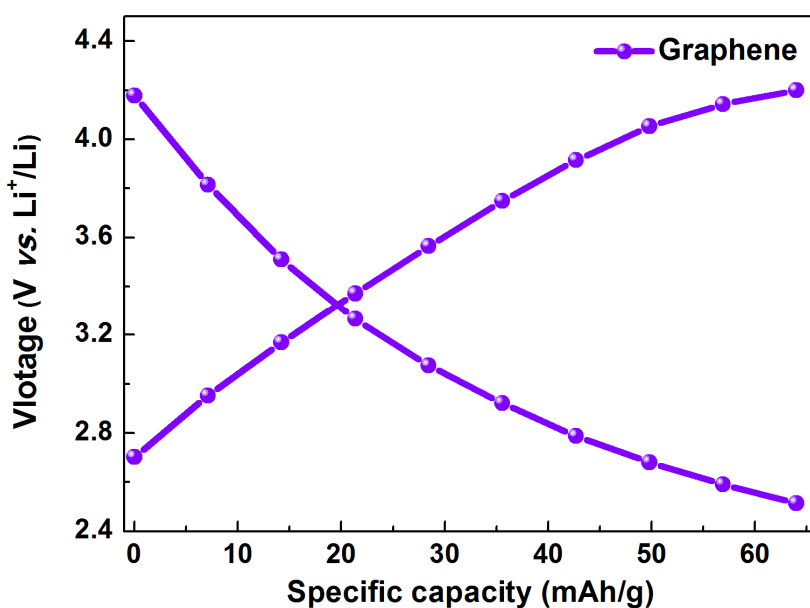


Fig. S7† Charge/discharge profiles of graphene electrode at 0.2C-0.2D.

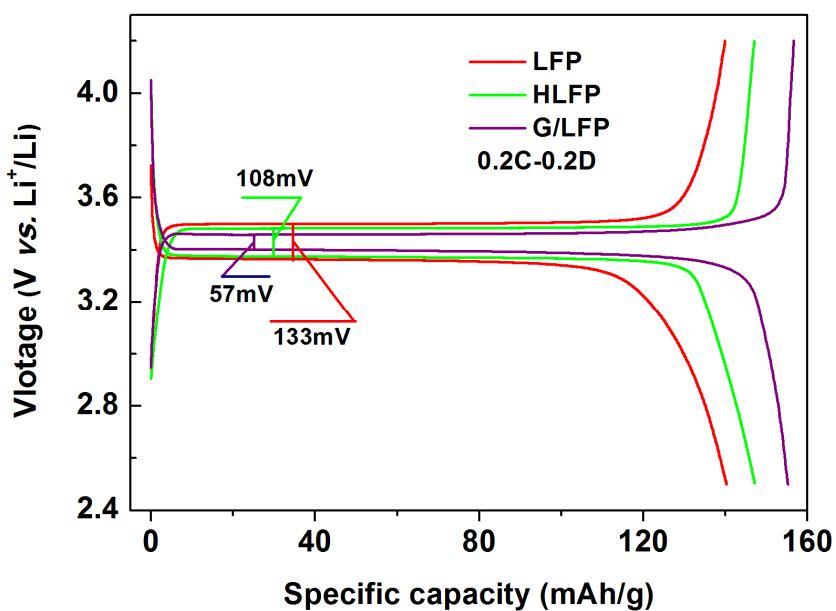


Fig. S8† The charge/discharge profiles of LFP, HLFP and G/LFP at current rates of 0.2C-0.2D.

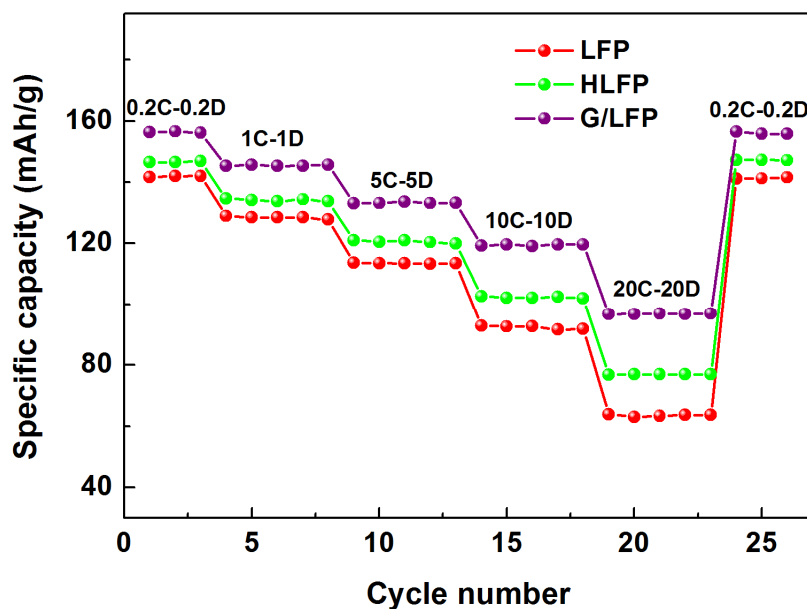


Fig. S9† The rate performance of LFP, HLFP and G/LFP from 0.2C-0.2D to 20C-20D.

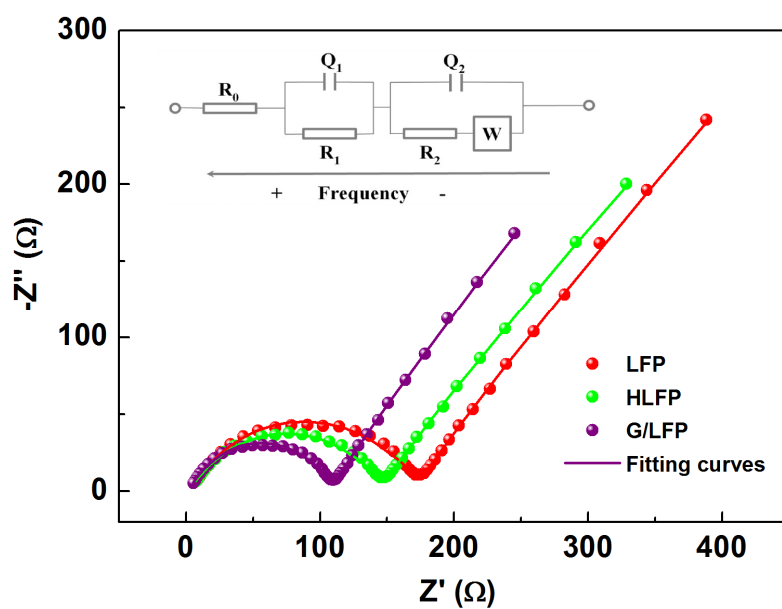


Fig. S10† The EIS plots and equivalent circuit of LFP, HLFP and G/LFP.

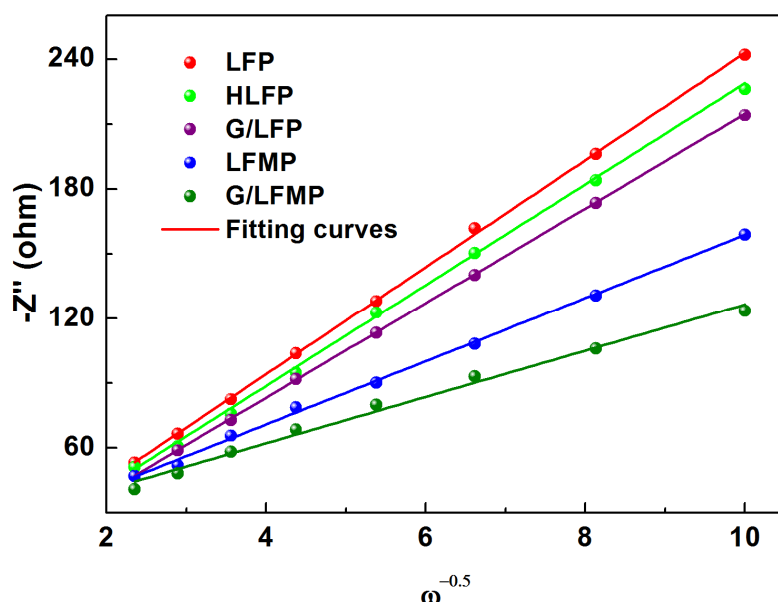


Fig. S11† The fitting curves of $-Z''$ and reciprocal square root of the angular frequency at low frequency region of LFP, HLFP, LFMP, G/LFP and G/LFMP.

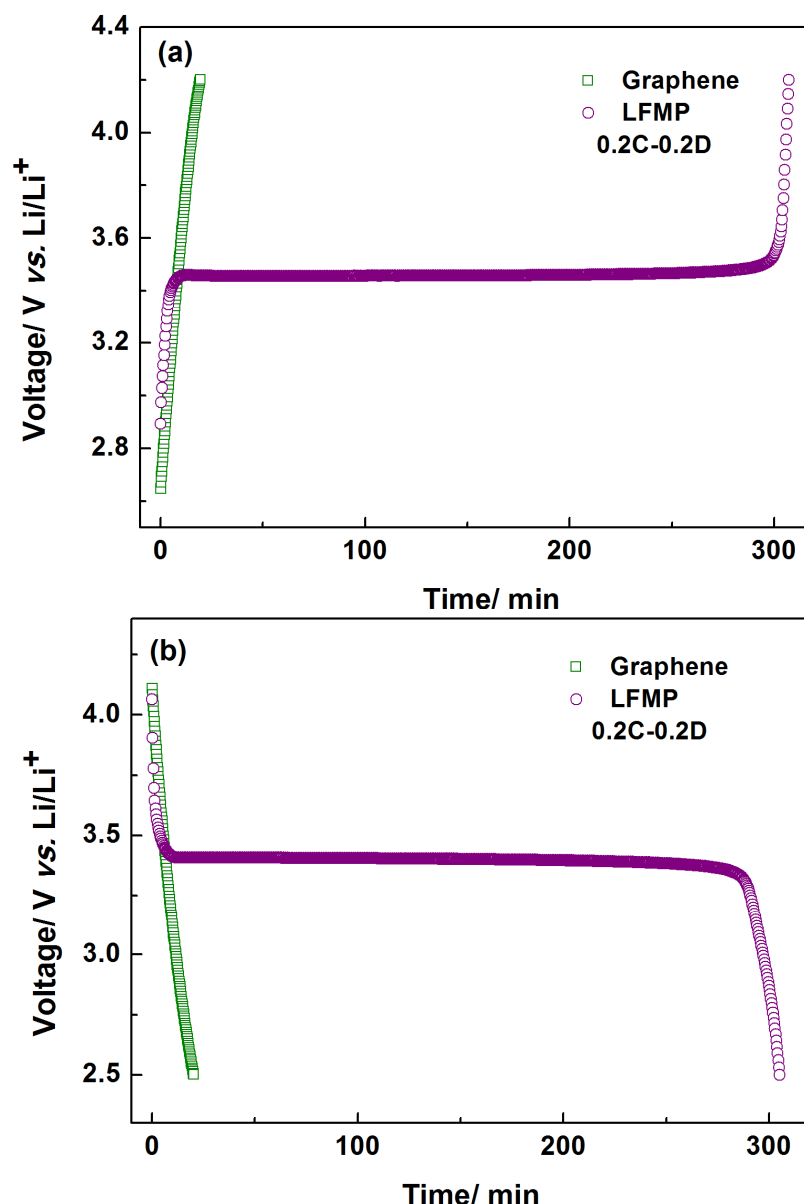


Fig. S12† Potential as a function of time of graphene electrode and LFMP electrode at 0.2C-0.2D for both charge (a) and discharge (b) processes.

Supplementary Material (ESI) for Nanoscale
 This journal is © Royal Society of Chemistry 2013

Table S1† Results of structural analysis obtained from XRD Rietveld refinement of samples LFP, LFMP, G/LFP and G/LFMP.

Samples	LFP	LFMP	G/LFP	G/LFMP
Doped ion radius/Å	0.74 (Fe^{2+})	0.65 (Mg^{2+})	0.74 (Fe^{2+})	0.65 (Mg^{2+})
Lattice constant/Å				
<i>a</i> /Å	10.3316	10.3286	10.3311	10.3275
<i>b</i> /Å	6.0097	6.0064	6.0089	6.0052
<i>c</i> /Å	4.6918	4.6895	4.6913	4.6883
<i>v</i> /Å ³	291.3130	290.9258	291.2291	290.7263
Lattice bond/Å				
Fe-O(1)×1	2.2083	2.2016	2.2079	2.2007
Fe-O(2)×1	2.1026	2.0975	2.1024	2.0967
Fe-O(3)×2	2.0605	2.0561	2.0607	2.0571
Fe-O(3)×2	2.2576	2.2436	2.2563	2.2432
Fe-O average	2.1573	2.1497	2.1568	2.1494
P-O(1)×1	1.4403	1.4206	1.4396	1.4235
P-O(2)×1	1.4935	1.4924	1.4941	1.4908
P-O(3)×2	1.4556	1.4562	1.4543	1.4537
P-O average	1.4631	1.4564	1.4627	1.4560
Li-O(1)×2	2.1541	2.1579	2.1539	2.1573
Li-O(2)×2	2.0879	2.0962	2.0881	2.0953
Li-O(3)×2	2.1806	2.1836	2.1782	2.1829
Li-O average	2.1409	2.1459	2.1407	2.1452
Reliability factors/%				
<i>R</i> _{wp}	6.63	5.96	6.35	5.81
<i>R</i> _p	4.67	3.96	4.03	4.56
<i>χ</i> ²	1.96	1.83	2.15	1.69

Table S2† The contents of LF(M)P, total carbon including sucrose-pyrolytic carbon and graphene, as well as electronic conductivities of the samples.

Samples	LF(M)P /wt.%	Total carbon/wt.%	Sucrose-pyrolytic carbon/wt.%	Graphene /wt.%	Electronic conductivity/S·cm ⁻¹
LFP	97.06	2.94	2.94	—	6.79×10^{-6}
HLFP	93.87	6.13	6.13	—	1.73×10^{-4}
LFMP	96.94	3.06	3.06	—	8.26×10^{-4}
G/LFP	94.04	5.96	~ 2.94 (similar to LFP)	~ 3.02	3.65×10^{-3}
G/LFMP	93.98	6.02	~ 3.06 (similar to LFMP)	~ 2.96	6.36×10^{-2}

Supplementary Material (ESI) for Nanoscale
This journal is © Royal Society of Chemistry 2013

Table S3† Elemental composition of the Mg²⁺ doping samples determined using ICP* (the other elements were not calculated).

Samples	Li	Fe	Mg	P
LFMP	0.99(2)	0.95(3)	0.04(7)	1
G/LFMP	0.99(4)	0.94(6)	0.05(2)	1

* Molar ratio based on element P as 1.

Table S4† The circuit parameters, D_{Li} , and σ of the samples.

Samples	R_θ/Ω	R_1/Ω	R_2/Ω	$D_{Li}/\text{cm}^2\cdot\text{s}^{-1}$	$\sigma/\Omega\cdot\text{s}^{-1/2}$
LFP	5.64	39.27	135.83	4.11×10^{-13}	24.79
HLFP	5.31	36.14	124.39	4.63×10^{-13}	23.36
LFMP	5.06	33.68	120.67	1.17×10^{-12}	14.66
G/LFP	3.87	28.93	91.85	5.25×10^{-13}	21.92
G/LFMP	3.69	26.75	52.76	2.19×10^{-12}	10.73